A modelling approach to explore the critical environmental parameters influencing the growth and establishment of the invasive seaweed Undaria pinnatifida in Europe

James T. Murphy, Mark P. Johnson, Frédérique Viard

A modelling approach to explore the critical environmental parameters influencing the growth and establishment of the invasive seaweed *Undaria pinnatifida* in Europe

James T. Murphy[a,b*], Mark P. Johnson[b], Frédérique Viard[a]

[a]Sorbonne Universités, UPMC Univ Paris 6, CNRS, UMR 7144, Department « Adaptation & Diversity in Marine Environment », Divco team, Station Biologique de Roscoff, Place Georges Teissier, 29680 Roscoff, France.

[b]Marine Environment Research Group, Ryan Institute, National University of Ireland Galway, Galway, Ireland.

*Corresponding author, mailing address: [a]Equipe Div&Co, UMR 7144 CNRS-UPMC, Station Biologique de Roscoff, Place Georges-Teissier CS 90074, 29688 Roscoff Cedex, France. Phone: +33 2 98 29 56 57. Email: jmurphy@sb-roscoff.fr

Abstract:

A key factor to determine the expansion dynamics and future distribution of non-native species is their physiological response to abiotic factors and their changes over time. For this study we developed a spatially explicit, agent-based model of population growth to represent the complex population dynamics of invasive marine macroalgae with heteromorphic biphasic life cycles. The model framework represents this complex life cycle by treating the individual developmental stages (gametophytes/sporophytes) as autonomous agents with unique behaviour/growth parameters. It was parameterised to represent a well-documented invasive algal species, the Asian kelp *Undaria pinnatifida*, and validated against field results from an *in situ* population in Brittany, France, showing good quantitative agreement in terms of seasonal changes in abundance/recruitment and growth dynamics. It was then used to explore how local environmental parameters (light availability, temperature and day length) affect the population dynamics of the individual developmental stages and the overall population growth. This type of modelling approach represents a promising tool for understanding the population dynamics of macroalgae from the bottom-up in terms of the individual interactions between the independent life history stages (both microscopic and macroscopic). It can be used to trace back the behaviour of the population as a whole to the underlying physiological and environmental processes impacting each developmental stage and give insights into the roles these play in invasion success.

Keywords:

Macroalgae; agent-based model; individual-based model; invasive species; seaweed; kelp; *Undaria pinnatifida*

1. Introduction:

The introduction and establishment of non-native plant and animal species can have a broad range of impacts on native species and community structure as well as economic consequences through the disruption of ecosystem services (Simberloff et al., 2013; Vilà et al., 2009). However, it is often difficult to predict the actual (and future) invasive behaviour under changing environmental conditions, since it is seldom possible to determine the source of an introduction with certainty, especially in marine environments (Rius et al., 2015). A further level of complexity comes from the fact that the response of introduced species to environmental factors may differ between the native and introduced ranges, as a consequence of trait plasticity (Davidson et al., 2011). A recent study of plant invaders pointed out an increased physiological tolerance of successful introduced species (Higgins and Richardson, 2014). Niche shift may thus be more common than previously assumed, which may complicate ecological-niche modelling efforts (Parravicini et al., 2015).

Seaweeds account for 20-29% of all non-native marine species in Europe and they are an important concern because of their role as primary producers in coastal ecosystems (Engelen et al., 2015; Schaffelke and Hewitt Chad, 2007; Schaffelke et al., 2006). One example of a notable invasive species on a global scale is the brown kelp *Undaria pinnatifida* (Harvey) Suringar, 1873 (Phaeophyceae: Laminariales). This has traditionally been cultivated in its native range of eastern Asia, including Japan, Korea and China (Ohno and Matsuoka, 1993; Shao-jun and Chao-yuan, 1996). However, in recent decades it has arisen as an invasive threat in Europe, North America and New Zealand among other places, due to human-mediated transport (Castric-Fey et al., 1993; Fletcher and Farrell, 1998; Floc'h et al., 1991; Grulois et al., 2011; Hay and Luckens, 1987; Silva et al., 2002; Voisin et al., 2005).

The order Laminariales (kelp) is characterised by a heteromorphic life history that consists of two distinct phases: a haploid gametophyte stage and a diploid sporophyte stage

(see Fig. 1) (Bessho and Iwasa, 2010; Clayton, 1988). Each stage has specific environmental requirements for optimal growth and development, in particular with respect to water temperature, light intensity and photoperiod (daily light:dark ratio) (Floc'h et al., 1991).

One key outcome of biological invasion studies has been to point out the role played by match-mismatch between the physiological requirements of the introduced species and the local environmental conditions. It is important to define the conditions under which introduced species expand (locally or spatially) in order to predict their fate. However, in many marine species, it is difficult to make predictions due to their complex life cycle and substantial variation in physiological traits. The purpose of this study was thus to propose a modelling approach that takes into account both the individual stages of the life cycle and their specific environmental requirements, when modelling the overall population dynamics.

An agent-based (or individual-based) modelling approach was chosen in order to be able to integrate data on the basic physiological properties of *U. pinnatifida* individuals into an overall model of population growth. This allows the individual life history stages (gametophytes/sporophytes) to be represented as autonomous agents and their behaviour/interactions to be explicitly described. This so-called bottom-up approach means that the emergent dynamics, at the population level, can be traced back to the individual components (Denny and Benedetti-Cecchi, 2012; Grimm and Railsback, 2005).

The main challenge in building an agent-based model of a complex biological system such as this is the ability to parameterise it. For this reason, a thorough review of the literature was first carried out in order to gather empirical data on the basic responses of the individual life stages of *U. pinnatifida* from a mechanistic point of view. We then tested the model for accuracy and robustness by comparing it with an empirical data set from a natural population in Brittany, France (Voisin, 2007). This step was critical as phenotypic plasticity is often assumed to be an important characteristic of invasive species. Finally, we used the

model to explore how some of the critical environmental parameters influence the population dynamics of the test species.

This type of low-level insight can help us to understand the role that climatic conditions play in the invasion dynamics of *U. pinnatifida* and other invasive macroalgae. The aim of this research was to develop a framework for exploring how direct and indirect effects on the life cycle and individual life history stages of macroalgae determine their population dynamics and invasive potential. This could enable better predictions about the potential future spread and range distribution of invasive seaweeds under changing climatic conditions. Furthermore, the agent-based approach means that heterogeneities in local environmental conditions, and between individual life history stages, can be explicitly accounted for in order to be able to predict the potential emergent dynamics at the population level.

2. The Model

The model was built upon a generic agent-based framework called CoastGEN, built in the C++ programming language, which has been developed to simulate populations of biological entities in a discrete two-dimensional environment (Murphy and Johnson, 2015). The advantages of this framework are that it is fully parallelisable (using domain decomposition and the Message Passing Interface) to take advantage of distributed computing architectures and it represents a robust and adaptable tool to simulate spatially and temporally heterogeneous phenomena (Gropp et al., 1996).

A detailed individual-based model of the life history of *U. pinnatifida* (including distinct microscopic gametophyte and macroscopic sporophyte stages) was built upon this basic framework for the purposes of this study. The input parameters used for the simulations in this paper are summarised in Table 1. Additional stochasticity is introduced into the model

by adding random individual variability when initialising each agent's parameters, using the Mersenne twister pseudo-random number generator (Matsumoto and Nishimura, 1998).

2.1. The environment

The coastal environment is represented as a discrete, two-dimensional grid with each grid element corresponding to 0.25 m^2 of surface area and periodic boundary conditions. This allows for heterogeneity in the environmental conditions and spatial distribution of organisms, as opposed to assuming a completely homogeneous, mixed environment. The maximum number of agents (gametophytes/sporophytes) that may occupy a lattice position can be specified by the user. For the purposes of the simulations in this paper, this value was set to 10^4, which was selected in order to avoid space limitations affecting the growth curves over the timescales involved in the simulations in this paper. To investigate the role of space limitations and competition in the natural environment, a more detailed model of frond structure and competition for light will need to be incorporated in future versions.

The availability of light in the water column is a function of the light attenuation coefficient for photosynthetically available radiation (K_{dPAR}) (Saulquin et al., 2013). This represents light attenuation in the water column due to backscattering of light caused by suspended matter and absorption by dissolved organic matter. Estimates of surface irradiance together with the K_{dPAR} are used to calculate the residual energy (I) available for photosynthesis at a given depth:

$$I = E(z) = E(0)e^{-zK_{dPAR}} \quad (1)$$

where z is depth (m), $E(0)$ is surface irradiance, and $E(z)$ is the irradiance energy available for photosynthesis at depth z. The average depth for the test simulations in this paper was set to 1.0 m. This was chosen in order to match the conditions from field surveys

of a natural population in Brest harbour which involved installing sampling panels that were suspended approximately a metre below the floating pontoons (Voisin, 2007).

At lower depths, growth becomes inhibited due to light limitation and peak recruitment is expected to decrease as a function of depth. This is why floating pontoons represent appropriate substrates for early colonisation by *U. pinnatifida* since they are maintained at a constant depth relative to the surface. Future work will involve more detailed analyses of the effects of depth and light attenuation on the growth of the various life history stages. However, for the purposes of this study, the depth was maintained at a constant value in order to represent optimal conditions for growth.

2.2. Gametophyte agents

Gametophytes are the microscopic haploid stages of the *U. pinnatifida* life cycle (see Fig. 1). In the model, their relative daily growth rate is calculated as a function of the water temperature, solar radiation, and number of day light hours. Experimental data is available in the literature for *U. pinnatifida* gametophytes growing under different temperature regimes (Morita et al., 2003a). To represent the effect of temperature on growth, a thermal performance curve (Stevenson et al., 1985) was fitted to this data (Fig. 2a, R^2>0.99):

$$RGR\_G_T = S\left[\frac{1}{(1 + K_1 e^{-K_2}(T_w - CT_{min})]}\right] \times \left[1 - e^{K_3(T_w - CT\max)}\right] \qquad (2)$$

where RGR_G_T is the relative growth rate in response to temperature, T_w is the current water temperature K_1, K_2 and K_3 are constants, CT_{min} and CT_{max} are the lower and upper critical temperature limits respectively, and S is a scaling factor.

Furthermore, it has been shown in studies that the growth rate of gametophytes is sensitive to changes in both solar irradiance and day length (Choi et al., 2005). This data set was used to generate a photosynthesis-irradiance curve by fitting the hyperbolic equation of

Jassby and Platt (1976) to empirical measurements of *U. pinnatifida* gametophytes by Choi et al. (2005) (Fig. 2b, R^2>0.99):

$$REG\_G_I = P_{max} \cdot (1 - \exp\left[-\alpha \cdot \frac{I - I_c}{P_{max}}\right]) \quad (3)$$

where REG_G_I is the relative effect of irradiance on the growth rate of the gametophyte agent, I is the current irradiance (μmol m^{-2} s^{-1}, calculated for a given depth by Equation 1 above), P_{max} is the maximum rate of photosynthesis, α is the slope of the curve and I_c is the compensation point (Jassby and Platt, 1976). Note that REG_G_I is expressed relative to a baseline condition (where irradiance = 40 μmol m^{-2} s^{-1} and day light (DL) hours = 12). The hyperbolic equation of Jassby & Platt was chosen because it has been extensively tested and applied to different species of marine organisms, including *U. pinnatifida* (Campbell et al., 1999; Harrison et al., 1985).

The data from Choi et al. (2005) was also used to calculate the relationship between day length (*d*, or day light hours) and the parameters P_{max} and α of the photosynthesis-irradiance curve. For α, there is a positive linear relationship with day length (R^2>0.99), whereas an exponential function was used to fit the data for P_{max} as a function of day length (R^2=0.95):

$$\alpha = 0.029d - 0.198 \quad (4)$$

$$P_{max} = 0.292e^{0.11d} \quad (5)$$

By incorporating these equations into the model it allows us to estimate the relative daily growth rate of the gametophyte agents (*RGR_G*) at any point in time as a function of the current temperature, irradiance and day length conditions:

$$RGR\_G = RGR\_G_T \times REG\_G_I \quad (6)$$

188 *2.3. Gametogenesis*

189 The maturation and production of gametes (or gametogenesis) by gametophytes, and
190 the subsequent fertilisation to form new sporophytes are important processes influenced by
191 external environmental cues. Experimental tests have demonstrated that there is a relationship
192 between day length/water temperature and the maturation of female gametophytes of *U.*
193 *pinnatifida* (Choi et al., 2005; Morita et al., 2003a).

194 The effect of temperature on the fertility of female gametophytes of *U. pinnatifida*
195 over the range 10-25^{o}C was explored by Morita et al. (2003a). They demonstrated a peak in
196 fertility at 10-15^{o}C with an approximately exponential decrease in fertility above that. A
197 simple logistic function was chosen to represent this as it showed a good fit against the data
198 over the temperature range explored (Fig. 2c, R^2=0.97):

$$RF_T = 1 - \left[\frac{1}{(1 + e^{-k(t-t_0)})}\right] \quad (7)$$

199 where RF_T is the relative fertility of the gametophytes in response to temperature, k is
200 the steepness of the curve, t is the current water temperature, and t_0 is the temperature at the
201 midpoint of the sigmoid.

202 The fertility of female gametophytes was also recorded by Choi et al. (2005) under
203 different day length regimes (8, 12 and 16 hours). A Weibull curve was fitted to this data
204 (R^2>0.99) in order to represent the effect of day length on the relative fertility (RF_{DL}) of the
205 gametophyte agents (Fig. 2d). This curve was chosen because of its relative simplicity and
206 flexibility (for example, it does not require any prior assumptions about symmetry in the
207 data).

208

209 *2.4. Sporophyte agents*

210 Sporophyte agents are modelled from their initial microscopic cellular scale up to an
211 eventual size of 1-3 metres (frond length), with growth represented as the relative daily

increase in the total length of the frond structure. This represents a particular modelling challenge due to the range of scales involved. Therefore, it was necessary to model the relative growth rate as a function of the length of the sporophyte. Studies from the literature were used to calculate the growth rate of sporophytes in different size classes (from microscopic sporophytes in culture to mature sporophytes 79 cm in length) (Choi et al., 2007; Pang and Lüning, 2004; Shao-jun and Chao-yuan, 1996). A power law functional relationship between the relative growth rate and the length of the sporophyte was estimated by fitting to this data (Fig. 3a, R^2=0.97):

$$RGR\_S_{base} = 3.615 l^{-0.407} \quad (8)$$

where l is the length of the sporophyte. This equation is used to calculate a baseline relative growth rate for sporophyte agents (RGR_S_{base}) under "default" environmental conditions (irradiance = 40 μmol m^{-2} s^{-1}, temperature = 15°C and day light (DL) hours = 12).

Furthermore, to account for the change in photosynthetic efficiency with increasing frond length (i.e. due to increasing thallus complexity/density and the proportion of differentiated cell types) the input parameters for the photosynthesis-irradiance curve of Jassby & Platt (Eq. 3) are expressed as functions of sporophyte length (Eq. 8-10). These functions were derived by fitting to data from Campbell et al. (1999) on macroscopic sporophytes and Choi et al. (2005) on microscopic gametophytes (R^2>0.99 for all three curves).

$$P_{max} = 0.4 \ln(l) - 0.596 \quad (9)$$

$$\alpha = 0.5 l^{-0.328} \quad (10)$$

$$I_c = 2.5 \ln(l) - 19.92 \quad (11)$$

To estimate the initial photosynthetic efficiency of microscopic sporophytes (i.e. immediately following fertilisation when the proportion of differentiated cell types is still low), data from studies of gametophytes had to be used. Nevertheless, this should be a

relatively good estimator of photosynthetic efficiency for the purposes of this model since the dry weight to fresh weight ratio of microscopic gametophytes and sporophytes would be expected to be similar due to the lack of differentiated cell types. The availability of equivalent data on cultured sporophytes would be preferable however.

Data from Pang and Lüning (2004) was used to characterise the effect of day length on the growth rate of sporophytes. They measured the time in weeks to maturity for sporophytes grown under different day length regimes and this was used to estimate the relative differences in growth rates. A hyperbolic curve (see Eq. 3) was then fitted to this data to predict the relative effect of day length on the growth rate (REG_S_{DL}) (Fig. 3b, R^2>0.99).

For temperature, a thermal performance curve was fitted to experimental data on sporophytes grown in water temperatures between 5-20ºC by Morita et al. (2003b), using the same approach described for the gametophyte agents above (see eq. 2). Figure 3c shows the results of fitting the curve to Morita's data through least squares regression (R^2=0.99) in order to represent the relative effect of temperature on the growth rate (REG_S_T). Finally, Fig. 3d shows an example of the photosynthesis-irradiance curve (REG_S_I) for an *U. pinnatifida* sporophyte as calculated directly by Campbell et al. (1999).

The relative daily growth rate of each sporophyte agent (RGR_S) is thus a function of the baseline growth rate and the relative effects of temperature, light and day length:

$$RGR\_S = RGR\_S_{base} \times REG\_S_T \times REG\_S_I \times REG\_S_{DL} \quad (12)$$

In order to test the growth algorithm described above, some initial validation tests were carried out on the predicted growth rates for sporophytes of different lengths versus observations from the literature. For example, in cultivation experiments (irradiance=100 μmol m^{-2} s^{-1}, temp=15ºC, DL=12h), Pang & Luning (2004) recorded average growth rates (measured as an increase in frond length) of 6-10 % per day among 3-4 week old sporophyte

recruits (length unspecified). Under similar conditions, the model predicts growth rates of 5.8-7% per day for 3-4 week old sporophytes (10-16 cm long). Similarly, Choi et al. (2007) recorded a relative growth rate (frond length) of 7.2% per day among a population of sporophytes with an average length of 79.06 cm. This compares to a model predicted growth rate of 6.9% (79 cm long, assuming light-saturated conditions).

Sporophytes agents die away naturally after reaching maturity and releasing all of their spores. However, the premature loss of sporophytes may also occur through potential random events (e.g. storms, grazers) which result in detachment/death. In fact, field studies in Brest harbour, France, have indicated that as much as 70% of all sporophyte recruits do not survive past their first month (Voisin, 2007). To account for this, an age to mortality curve (Weibull function) was calculated and fitted to the data from Brest harbour to determine the probability of premature death as a function of the age of the sporophyte (Fig. 4a).

2.5. Spore Release

Mature sporophytes are characterised by a distinct sporophyll structure at the base of their stipe in which the spores are formed. The mean size at maturity calculated for a population in Brest harbour, France was 32.66 cm (Voisin, 2007). This is used in the model to determine the mean minimum size at which spore release can occur. The release of spores by mature sporophytes is thought to be a temperature-dependent event (Saito, 1975). Suto (1952) recorded the average (10-day) sea water temperatures and the presence/absence of shedding among *U. pinnatifida* sporophytes in Japan (Suto, 1952). We used their original data to plot the frequency of spore release versus temperature and fitted a logistic function to this (Fig. 4b, $R^2>0.99$).

For the test simulations in this paper, the mean spore release rate per individual sporophyte agent was set to 2.0×10^7 spores $hour^{-1}$ and total spore production in a season is

10^{10} spores sporophyte^{-1}. This is within the range of estimates for the rate of spore release (1.0×10^7 - 1.4×10^8 spores h^{-1}) and the total spore production (>10^9) for *U .pinnatifida* from the literature (Schaffelke et al., 2005; Suto, 1950). Once released, they are represented as simple particles subject to a discretised implementation of Fick's First Law of diffusion for dispersal across a lattice environment (Ginovart et al., 2002). Water currents are not explicitly simulated, but in terms of local population dynamics a simple diffusion algorithm is thought to be sufficient due to the short lifespan of spore particles in the water column (Thiébaut et al., 1998).

Experimental studies have shown that *U. pinnatifida* spores can lose their fixing ability within hours of release and stop swimming within 3 days (Forrest et al., 2000; Suto, 1950). Therefore, they were assigned a relatively short half-life of 24 hours in the simulations. A gametophyte agent is formed when a spore comes into contact with a suitable substrate for attachment. In the model, this process is represented as a simple stochastic process where the probability of recruitment of new gametophytes ($P_{recruit}$) is a function of the number of spores occupying the lattice position ij (s_{ij}) at that point in time and a user-defined probability of attachment/germination on the substrate (A_{substr}):

$$P_{recruit} = A_{substr} s_{ij} \quad (13)$$

3. Results & Discussion:

3.1. Model validation

Simulations were carried out using environmental parameters (light, temperature and day length) representative of Brest harbour, France, in order to validate the model against real-world data collected by researchers at the Station Biologique de Roscoff, France. Surface water temperature data for the port of Brest (2003-06) were obtained from a SOMLIT

306 (Service d'Observation en Milieu Littoral, INSU-CNRS, Brest, http://somlit-db.epoc.u-
307 bordeaux1.fr) buoy situated a few hundred metres from the marina (Voisin, 2007).
308 Meanwhile, sample mean global solar irradiance data for the region were obtained using the
309 CalSol online application (Institut National de L'Energie Solaire, CEA-CNRS).

310 Figure 5 shows model predictions for the overall sporophyte population growth of an
311 *U. pinnatifida* invasion in a harbour setting (for raw data, see Table 1, (Murphy et al.,
312 (submitted))). The model displays an annual pattern of growth and decay characteristic of *U.*
313 *pinnatifida* populations in nature, in response to seasonal variations in light and temperature
314 levels. For validation purposes, this was compared to real-world field results from the port of
315 Brest in France during the 2005/06 growing season (Voisin, 2007): During this field
316 experiment, 64 aluminium panels were set-up one metre below the surface, a depth optimal
317 for the recruitment of the study species, and the settlement and length of each individual was
318 recorded every month.

319 The raw data was first normalised to express the monthly abundance/recruitment
320 values for the sporophytes relative to their peak annual abundance/recruitment respectively
321 (see Tables 2-3, (Murphy et al., (submitted))). This means that all monthly abundance values
322 for a growing season (Aug-July) were expressed relative to the peak abundance in that year
323 (usually in April). This was done in order to avoid bias in the results due to differences in
324 population size and to focus on the relative seasonal variation in abundance/recruitment due
325 to environmental effects.

326 The model results and field data were then plotted against each other in terms of
327 overall abundance data and monthly recruitment rates (Fig. 6a & b). The R^2 values were 0.84
328 and 0.85 when comparing the model predictions and the real-world measurements for total
329 abundance and monthly recruitment respectively over the course of the 12 months. Some
330 variation from the real-world results is to be expected since factors such as competition and

self-shading were not taken into account. Future work will involve extending the base model to incorporate intra- and inter-specific competition for light/space.

Figure 6b shows the monthly recruitment rate (i.e. appearance of new sporophytes >5 cm in length) for Brest harbour compared with the model predictions. The model matches closely the seasonal pattern of growth observed in the real-world populations. The one exception is in November when the model over-predicts the rate of recruitment. Possible explanations for this include seasonal changes in the turbidity of the water affecting the growth of young sporophytes or increased mortality due to winter storm activity that year.

The predicted life expectancy and age to maturity for *U. pinnatifida* sporophytes were also compared with field records from Brest (Fig. 7). There is good quantitative agreement between the model predictions and field measurements for life expectancy, age to maturity and duration of the mature phase respectively. This indicates that the physiological responses to environmental factors of the local population of *U. pinnatifida* match closely with predictions based on studies of individuals in its native range of eastern Asia.

Voisin (2007) also investigated the important relationship between water temperature and the recruitment of sporophytes. Previous studies in California, USA, had identified recruitment pulses in *U. pinnatifida* populations associated with drops in ocean temperature 2 months prior to the recruitment (Thornber et al., 2004). Therefore, to investigate if the model reproduced this pattern the predicted rate of recruitment was plotted against the water temperature two months prior, and compared with similar field results from Brest. As can be seen in Figure 8, there is good overlap between model predictions and the real-world data (for raw data, see Table 4, (Murphy et al., (submitted))). They both show increased recruitment at lower temperatures, which agrees with data from the literature indicating significantly higher recruitment of sporophytes at temperatures below 15^{o}C (Thornber et al., 2004; Voisin, 2007).

It must be noted that apart from the use of a scaling factor, no attempt to fit the model parameters to the Brest population was made. The model input parameters were solely based on experimental records from various studies in the literature often involving geographically disparate populations of *U. pinnatifida* in their native range. Interestingly, the fact that the Brest population behaves similarly to the model predictions may indicate that relatively limited phenotypic adaptation has occurred in the local Brittany populations as compared to its native range, meaning that this species may be pre-adapted to a large set of environmental conditions, for the factors considered here. In this case, abiotic factors seem to be the dominant factor in influencing the local population dynamics. However, since *U. pinnatifida* is a recent introduction to Brittany, there is the possibility that future adaptation to the new environment may play an important role in determining its continued spread in the region.

3.2. Response to environmental parameters

The next step was to explore the underlying system dynamics and critical parameters that contribute to the observed patterns of growth predicted by the model. To achieve this, the responses of the various developmental stages of *U. pinnatifida* to three key environmental parameters (light, temperature, and day length) were investigated using the model. Figures 9-11 represent the raw simulation output expressed in terms of these three environmental variables. All the plots come from an identical simulation run over the course of 56 months in order to exclude any variation due to differences in the initial conditions. By dissecting the model output like this, it is possible to gain insights into the underlying mechanisms for the observed patterns of population growth.

Figure 9 plots the relationship between water temperature and the growth/fertility of *U. pinnatifida* agents in the model. In the case of both the gametophyte and sporophyte stages of the life cycle, the growth rate is moderately positively correlated with water temperature

(Fig. 9a-b, R^2=0.65 & 0.7 respectively). However, temperature does not appear to play an important role in influencing gametophyte fertility, with a minor negative correlation predicted (Fig. 9c, R^2=0.4). This is because the water temperature in Brest harbour rarely exceeds a value that would be expected to inhibit the maturation of gametophytes (>21ºC). However, this may play a greater role in influencing the population dynamics under scenarios of increasing sea water temperatures in the study area (Brittany) in the future (Gallon et al., 2014). Finally, spore release by mature sporophytes primarily occurs at higher water temperatures >10ºC (Fig. 9d). This agrees with field studies from the literature which suggested a critical minimum temperature value for spore release of approximately 12-14ºC (Saito, 1975; Suto, 1952).

In the case of day light hours and solar radiation, these also play a key role in influencing the population dynamics of *U. pinnatifida* (Fig. 10 & 11). The model results indicate a positive correlation between day light hours/solar radiation and the growth rate of gametophytes (Fig. 10a & 11a: R^2=0.82 & 0.74 respectively). Similarly, for sporophytes, there is a moderate positive correlation (Fig. 10b & 11b: R^2=0.6 & 0.62 respectively). In contrast, the fertility of gametophytes is negatively correlated with day length and light availability (Fig. 10c & 11c: R^2=0.87 & 0.77 respectively). These results suggest that gametogenesis and new sporophyte formation is adapted to occur during the shorter days of winter. Conversely, there is no clear relationship between spore release and either day length or solar radiation (R^2<0.1, Figs. 10d & 11d). This is because the model does not assume any relationship between these variables and spore release as there is no clear data from the literature of a direct causal relationship.

The different patterns of response to environmental parameters between the life history stages (particularly gametophyte fertility, gametophyte growth rates and sporophyte growth rates) in response to the environmental parameters is an important consideration when

attempting to explain the patterns of growth observed in populations of *U. pinnatifida* in the field. It is necessary to take into account these complex interactions in order to build up an accurate view of the invasion dynamics but this is often overlooked in population studies that focus on the macroscopic stages of the life cycle alone. Furthermore, these types of interactions are common in other species of macroalgae that exhibit dimorphic life cycles. Therefore, a modelling approach which explicitly takes into account the differing responses of the individual life stages may be a useful tool for understanding the complex non-linear dynamics of macroalgal populations in general.

The results in this paper illustrate how the characteristic seasonal growth patterns observed among populations of *U. pinnatifida* in Brest harbour are dictated by the differing responses of the individual life history stages to environmental parameters: Gametophytes mature and reproduce to form new sporophytes during the shorter days of the winter when light availability is lowest. They reach maturity in the spring and release their spores in the early summer when light availability is at its peak, before dying out gradually during the spring and summer months. The population dynamics of the gametophyte stages in field populations are less well understood. However, the model predicts that the density of gametophytes is expected to peak in the summer months but there is a delay before maturity is reached during the autumn when appropriate conditions (day length/solar irradiance) are present.

The individual-based modelling approach allows us to make quantitative predictions about the temporal and spatial dynamics affecting this seasonal schedule using basic physiological data on the species. It has been suggested that the heteromorphic life cycle of macroalgal species such as *U. pinnatifida* may have evolved in response to seasonal changes in temperate climates (Bessho and Iwasa, 2009). Therefore, it is important to take into

account the ecophysiological responses of the individual life history stages when attempting to make predictions about the responses of the population as a whole.

The individual-based approach allows us to treat the life history stages as independent entities and to connect the local interactions at the individual-scale to the overall population dynamics. A greater understanding of the mechanistic basis for these responses could allow predictions about how populations will respond to changing environmental conditions in the future (such as increasing sea water temperatures) and the potential for future range expansion in Europe and other regions of the world. There is an extra computational burden associated with the IBM approach and it is more dependent on empirical knowledge compared to simpler state variable modelling approaches. However, by using appropriate aggregation of parameters in order to simplify the model, and cognizant of its limitations, it can be a useful approach to supplement, rather than supplant, existing theoretical approaches, such as metapopulation models, when local interactions play an important role (McCauley et al., 1993).

In addition, the IBM approach provides a framework to understand how processes at the individual level and local interactions affect invasion success. It allows spatial heterogeneity (or patches) to be generated both “internally”, by the interactions and movements of the organisms, as well as imposed “externally” (for example, by specifying the structure of a harbour with different substrates, currents etc.). This allows the effects of local rules, for migration or diffusion between or among patches, on population dynamics to be assessed. It also allows one to differentiate the responses of the gametophyte and sporophyte stages and to isolate the key factors that limit/promote the population growth/fitness under a given set of environmental conditions. This can help to inform strategies for control/eradication of invasive populations by identifying susceptible stages in the life cycle

schedule and the timing of intervention, or to assess the risk for spread and establishment of the species in a region.

4. Conclusions & Future Work:

We present a novel agent-based modelling framework for simulating marine macroalgal species taking into account their complex biphasic life histories. Initial validation results indicate that the model can accurately predict the growth dynamics of an *in situ* population of invasive seaweed (*U. pinnatifida*, in Brest harbour, France) and give insights into the underlying population dynamics that contributed to its establishment. This type of modelling approach represents a promising tool for understanding the effects of changing environmental conditions (both temporal: e.g. climate change; and spatial: e.g. by range expansion) on the growth dynamics and distribution of invasive seaweed species. Moreover, through building a mechanistic representation of the important life history stages of the species, and modelling their basic interactions at an individual level, it is possible to build up a more complete understanding of the underlying dynamics driving their spread and establishment. This can have applications in terms of informing control strategies for invasive populations and risk assessment for the potential spread and establishment of non-native species.

Future work will involve extending the model to represent more complex spatial and temporal patterns of invasion in order to be able to explore the impact of these factors on invasion dynamics. A detailed competition model will be incorporated to represent the potential interactions between different algal species and local ecosystem dynamics. This individual-based approach could also enable investigations into more long term processes such as the role of phenotypic/genotypic variation and evolutionary selective pressures on invasion dynamics.

Acknowledgements:

This research is supported by an Irish Research Council ELEVATE international career development fellowship, co-funded by Marie Curie Actions under the European Union's Seventh Framework Programme. The field data presented here, which were collected in Brest, were obtained as part of the PhD thesis of Marie Voisin who benefitted from a Ph.D. fellowship ("Renouvellement des Compétences" Program) from the Region Bretagne. MV and FV are thankful to the many people from the Department AD2M of the Station Biologique de Roscoff who provided help for the surveys carried out in the field.

References:

Bessho, K., and Iwasa, Y., 2009. Heteromorphic and isomorphic alternations of generations in macroalgae as adaptations to a seasonal environment. Evolutionary Ecology Research 11, 691-711.

Bessho, K., and Iwasa, Y., 2010. Optimal seasonal schedules and the relative dominance of heteromorphic and isomorphic life cycles in macroalgae. Journal of Theoretical Biology 267, 201-212.

Campbell, S.J., Bité, J.S., and Burridge, T.R., Seasonal Patterns in the Photosynthetic Capacity, Tissue Pigment and Nutrient Content of Different Developmental Stages of *Undaria pinnatifida* (Phaeophyta: Laminariales) in Port Phillip Bay, South-Eastern Australia, Botanica Marina, Vol. 42. 1999, pp. 231.

Castric-Fey, A., Girard, A., and L'Hardy-Halos, M.T., The Distribution of *Undaria pinnatifida* (Phaeophyceae, Laminariales) on the Coast of St. Malo (Brittany, France), Botanica Marina, Vol. 36. 1993, pp. 351.

Choi, H., Kim, Y., Lee, S., and Nam, K., 2007. Growth and reproductive patterns of *Undaria pinnatifida* sporophytes in a cultivation farm in Busan, Korea. Journal of Applied Phycology 19, 131-138.

Choi, H., Kim, Y., Lee, S., Park, E., and Nam, K., 2005. Effects of daylength, irradiance and settlement density on the growth and reproduction of *Undaria pinnatifida* gametophytes. Journal of Applied Phycology 17, 423-430.

Clayton, M.N., Evolution and Life Histories of Brown Algae, Botanica Marina, Vol. 31. 1988, pp. 379.

Davidson, A.M., Jennions, M., and Nicotra, A.B., 2011. Do invasive species show higher phenotypic plasticity than native species and, if so, is it adaptive? A meta-analysis. Ecology Letters 14, 419-431.

Denny, M., and Benedetti-Cecchi, L., 2012. Scaling Up in Ecology: Mechanistic Approaches. Annual Review of Ecology, Evolution, and Systematics 43, 1-22.

Engelen, A.H., Serebryakova, A., Ang, P., Britton-Simmons, K., Mineur, F., Pedersen, M.F., Arenas, F., Fernández, C., Steen, H., Svenson, R., Pavia, H., Toth, G., Viard, F., and Santos, R., Circumglobal invasion by the brown seaweed *Sargassum muticum*, Oceanography and Marine Biology: An Annual Review, Vol. 53. Taylor & Francis 2015, pp. 81-126.

Fletcher, R.L., and Farrell, P., 1998. Introduced brown algae in the North East Atlantic, with particular respect to *Undaria pinnatifida* (Harvey) suringar. Helgoländer Meeresuntersuchungen 52, 259-275.

Floc'h, J.Y., Pajot, R., and Wallentinus, I., 1991. The Japanese brown alga *Undaria pinnatifida* on the coast of France and its possible establishment in European waters. Journal du Conseil: ICES Journal of Marine Science 47, 379-390.

Forrest, B.M., Brown, S.N., Taylor, M.D., Hurd, C.L., and Hay, C.H., 2000. The role of natural dispersal mechanisms in the spread of *Undaria pinnatifida* (Laminariales, Phaeophyceae). Phycologia 39, 547-553.

Gallon, R.K., Robuchon, M., Leroy, B., Le Gall, L., Valero, M., and Feunteun, E., 2014. Twenty years of observed and predicted changes in subtidal red seaweed assemblages along a biogeographical transition zone: inferring potential causes from environmental data. Journal of Biogeography 41, 2293-2306.

Ginovart, M., López, D., and Valls, J., 2002. INDISIM, An Individual-based Discrete Simulation Model to Study Bacterial Cultures. Journal of Theoretical Biology 214, 305-319.

Grimm, V., and Railsback, S.F., 2005. Individual-based Modeling and Ecology. Princeton University Press.

Gropp, W., Lusk, E., Doss, N., and Skjellum, A., 1996. A high-performance, portable implementation of the MPI message passing interface standard. Parallel Computing 22, 789-828.

Grulois, D., Lévêque, L., Viard, F., Frangoudes, K., and Valero, M., 2011. Mosaic genetic structure and sustainable establishment of the invasive kelp *Undaria pinnatifida* within a bay (Bay of St-Malo, Brittany). CBM-Cahiers de Biologie Marine 52, 485.

Harrison, W.G., Platt, T., and Lewis, M.R., 1985. The Utility of Light-Saturation Models for Estimating Marine Primary Productivity in the Field: A Comparison with Conventional "Simulated" In Situ Methods. Canadian Journal of Fisheries and Aquatic Sciences 42, 864-872.

Hay, C.H., and Luckens, P.A., 1987. The Asian kelp *Undaria pinnatifida* (Phaeophyta: Laminariales) found in a New Zealand harbour. New Zealand Journal of Botany 25, 329-332.

Higgins, S.I., and Richardson, D.M., 2014. Invasive plants have broader physiological niches. Proceedings of the National Academy of Sciences 111, 10610-10614.

Jassby, A.D., and Platt, T., 1976. Mathematical formulation of the relationship between photosynthesis and light for phytoplankton. Limnology and Oceanography 21, 540-547.

Matsumoto, M., and Nishimura, T., 1998. Mersenne twister: a 623-dimensionally equidistributed uniform pseudo-random number generator. ACM Trans. Model. Comput. Simul. 8, 3-30.

McCauley, E., Wilson, W.G., and de Roos, A.M., 1993. Dynamics of Age-Structured and Spatially Structured Predator-Prey Interactions: Individual-Based Models and Population-Level Formulations. The American Naturalist 142, 412-442.

Morita, T., Kurashima, A., and Maegawa, M., 2003a. Temperature requirements for the growth and maturation of the gametophytes of *Undaria pinnatifida* and *U. undarioides* (Laminariales, Phaeophyceae). Phycological Research 51, 154-160.

566 Morita, T., Kurashima, A., and Maegawa, M., 2003b. Temperature requirements for the
567 growth of young sporophytes of *Undaria pinnatifida* and *Undaria undarioides*
568 (Laminariales, Phaeophyceae). Phycological Research 51, 266-270.
569 Murphy, J.T., and Johnson, M.P., 2015. A theoretical analysis of the Allee effect in wind-
570 pollinated cordgrass plant invasions. Theoretical Population Biology 106, 14-21.
571 Murphy, J.T., Johnson, M.P., and Viard, F., (submitted). Abundance and recruitment data for
572 *Undaria pinnatifida* in Brest harbour, France: Model versus field results. Data in
573 Brief.
574 Ohno, M., and Matsuoka, M., 1993. Undaria cultivation 'wakame'. Seaweed cultivation and
575 marine ranching. Kanagawa International Fisheries Training Center Japan
576 International Cooperative Agency, Yokosuka, 41-49.
577 Pang, S., and Lüning, K., 2004. Photoperiodic long-day control of sporophyll and hair
578 formation in the brown alga *Undaria pinnatifida*. Journal of Applied Phycology 16,
579 83-92.
580 Parravicini, V., Azzurro, E., Kulbicki, M., and Belmaker, J., 2015. Niche shift can impair the
581 ability to predict invasion risk in the marine realm: an illustration using Mediterranean
582 fish invaders. Ecology Letters 18, 246-253.
583 Rius, M., Turon, X., Bernardi, G., Volckaert, F.M., and Viard, F., 2015. Marine invasion
584 genetics: from spatio-temporal patterns to evolutionary outcomes. Biological
585 Invasions 17, 869-885.
586 Saito, Y., 1975. Undaria. Advance of Phycology in Japan, Junk Publishers, The Hague, 304-
587 320.
588 Saulquin, B., Hamdi, A., Gohin, F., Populus, J., Mangin, A., and d'Andon, O.F., 2013.
589 Estimation of the diffuse attenuation coefficient KdPAR using MERIS and
590 application to seabed habitat mapping. Remote Sensing of Environment 128, 224-233.
591 Schaffelke, B., and Hewitt Chad, L., Impacts of introduced seaweeds, Botanica Marina, Vol.
592 50. 2007, pp. 397.
593 Schaffelke, B., Campbell, M.L., and Hewitt, C.L., 2005. Reproductive phenology of the
594 introduced kelp Undaria pinnatifida (Phaeophyceae, Laminariales) in Tasmania,
595 Australia. Phycologia 44, 84-94.
596 Schaffelke, B., Smith, J.E., and Hewitt, C.L., 2006. Introduced macroalgae - A growing
597 concern. Journal of Applied Phycology 18, 529-541.
598 Shao-jun, P., and Chao-yuan, W., 1996. Study on gametophyte vegetative growth of *Undaria*
599 *pinnatifida* and its applications. Chinese Journal of Oceanology and Limnology 14,
600 205-210.
601 Silva, P., Woodfield, R., Cohen, A., Harris, L., and Goddard, J.R., 2002. First Report of the
602 Asian kelp *Undaria pinnatifida* in the Northeastern Pacific Ocean. Biological
603 Invasions 4, 333-338.
604 Simberloff, D., Martin, J.-L., Genovesi, P., Maris, V., Wardle, D.A., Aronson, J.,
605 Courchamp, F., Galil, B., García-Berthou, E., Pascal, M., Pyšek, P., Sousa, R.,
606 Tabacchi, E., and Vilà, M., 2013. Impacts of biological invasions: what's what and the
607 way forward. Trends in Ecology & Evolution 28, 58-66.
608 Stevenson, R.D., Peterson, C.R., and Tsuji, J.S., 1985. The thermal dependence of
609 locomotion, tongue flicking, digestion, and oxygen consumption in the wandering
610 garter snake. Physiological Zoology, 46-57.
611 Suto, S., 1950. Studies on shedding, swimming and fixing of the spores of seaweeds. Bulletin
612 of the Japanese Society of Scientific Fisheries 16, 1-9.
613 Suto, S., 1952. On shedding of zoospores in some algae of Laminariaceae-2. Bull. Jap. Soc.
614 scient. Fish 18, 1-5.

615 Thiébaut, E., Lagadeuc, Y., Olivier, F., Dauvin, J.C., and Retière, C., 1998. Do
616 hydrodynamic factors affect the recruitment of marine invertebrates in a macrotidal
617 area? The case study of Pectinaria koreni (Polychaeta) in the Bay of Seine (English
618 Channel). Hydrobiologia 375-376, 165-176.
619 Thornber, C.S., Kinlan, B.P., Graham, M.H., and Stachowicz, J.J., 2004. Population ecology
620 of the invasive kelp Undaria pinnatifida in California: environmental and biological
621 controls on demography. Marine Ecology Progress Series 268, 69-80.
622 Vilà, M., Basnou, C., Pyšek, P., Josefsson, M., Genovesi, P., Gollasch, S., Nentwig, W.,
623 Olenin, S., Roques, A., Roy, D., and Hulme, P.E., 2009. How well do we understand
624 the impacts of alien species on ecosystem services? A pan-European, cross-taxa
625 assessment. Frontiers in Ecology and the Environment 8, 135-144.
626 Voisin, M., Les processus d'invasions biologiques en milieu côtier marin: le cas de l'algue
627 brune *Undaria pinnatifida*, cultivée et introduite à l'échelle mondiale (PhD diss.),
628 Paris 6, France 2007.
629 Voisin, M., Engel, C.R., and Viard, F., 2005. Differential shuffling of native genetic diversity
630 across introduced regions in a brown alga: Aquaculture vs. maritime traffic effects.
631 Proceedings of the National Academy of Sciences of the United States of America
632 102, 5432-5437.
633
634
635

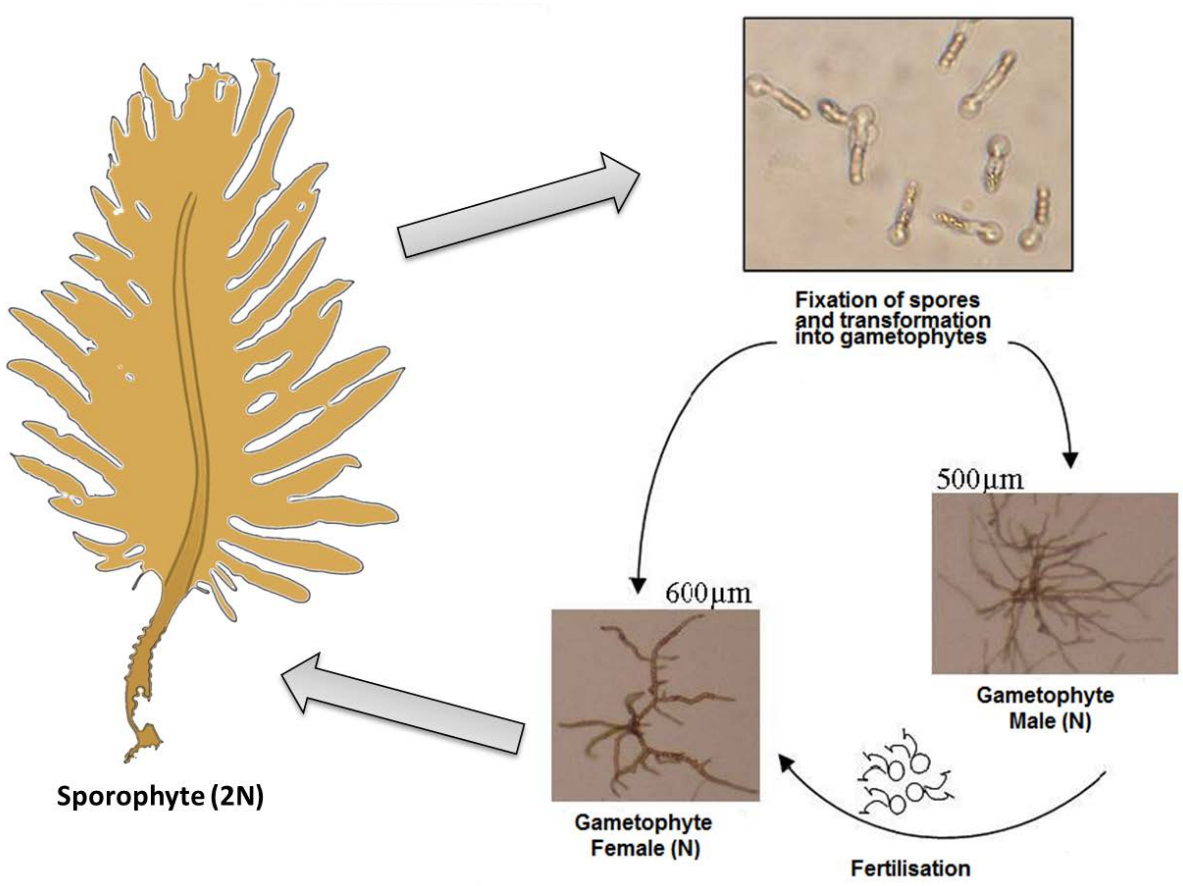

636

637 **Fig. 1:** Heteromorphic life cycle of *Undaria pinnatifida* consisting of microscopic haploid
638 (N) gametophyte stages which reproduce sexually to form the diploid (2N) sporophyte stage
639 (1-3 m in length). Photos: Daphné Grulois-Station Biologique Roscoff.

640

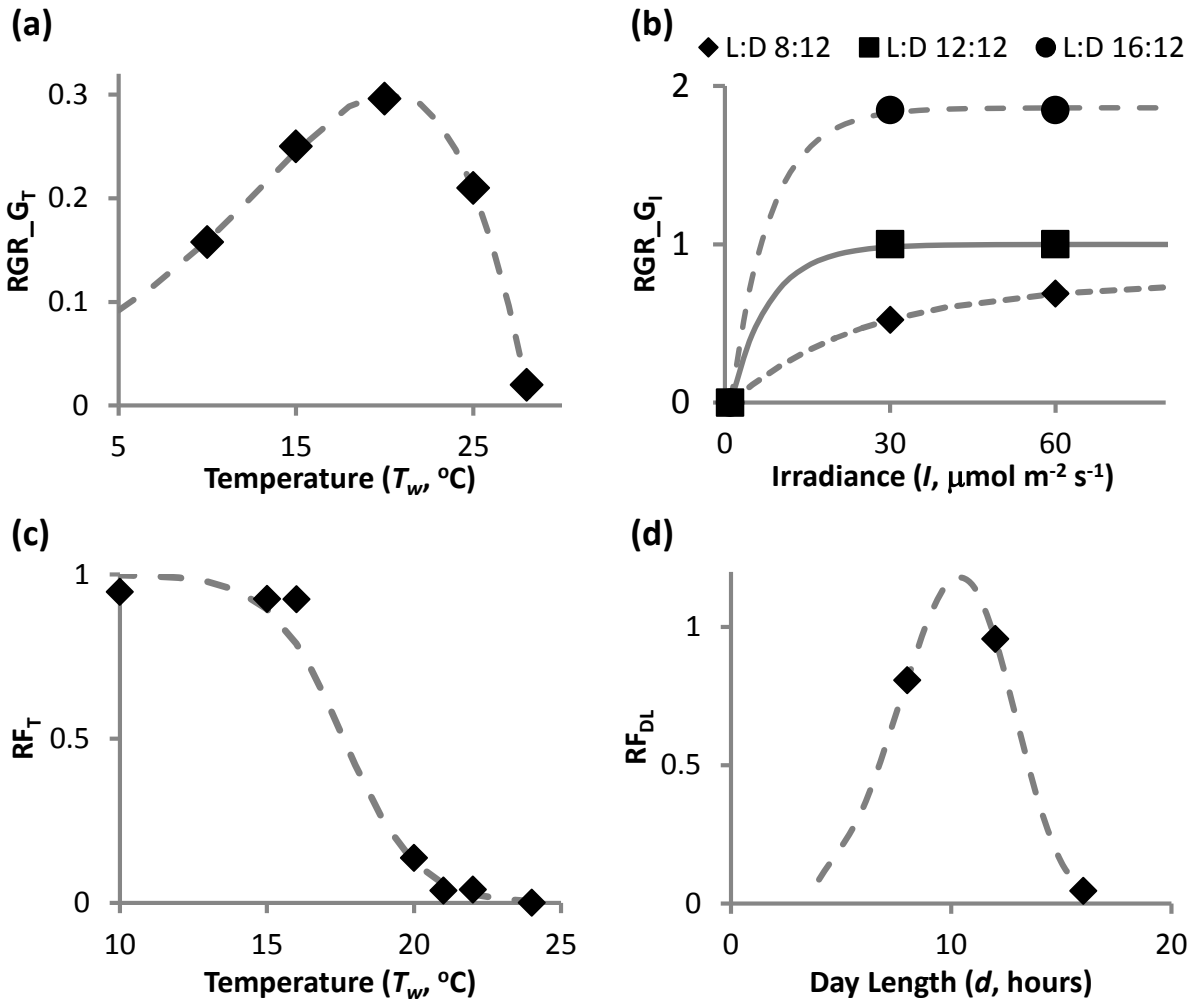

641
642

643 **Fig. 2:** Response of gametophyte agents to environmental parameters. **(a)** Relative growth
644 rate in response to temperature (RGR_G_T). Thermal performance curve fitted to data from
645 Morita et al. (2003) (R^2>0.99). **(b)** Relative effect of solar irradiance and day length (day
646 light hours) on growth rate (REG_G_I): Hyperbolic function fitted to data from Choi et al.
647 (2005) (R^2>0.99 for all curves). **(c)** Relative effect of temperature on fertility (RF_T): Logistic
648 function fitted to data from Morita et al. (2003) and Choi et al. (2005) (R^2=0.97). **(d)** Relative
649 effect of day length on fertility (RF_{DL}): Weibull distribution fitted to data from Choi et al.
650 (2005) (R^2=1.0).

651

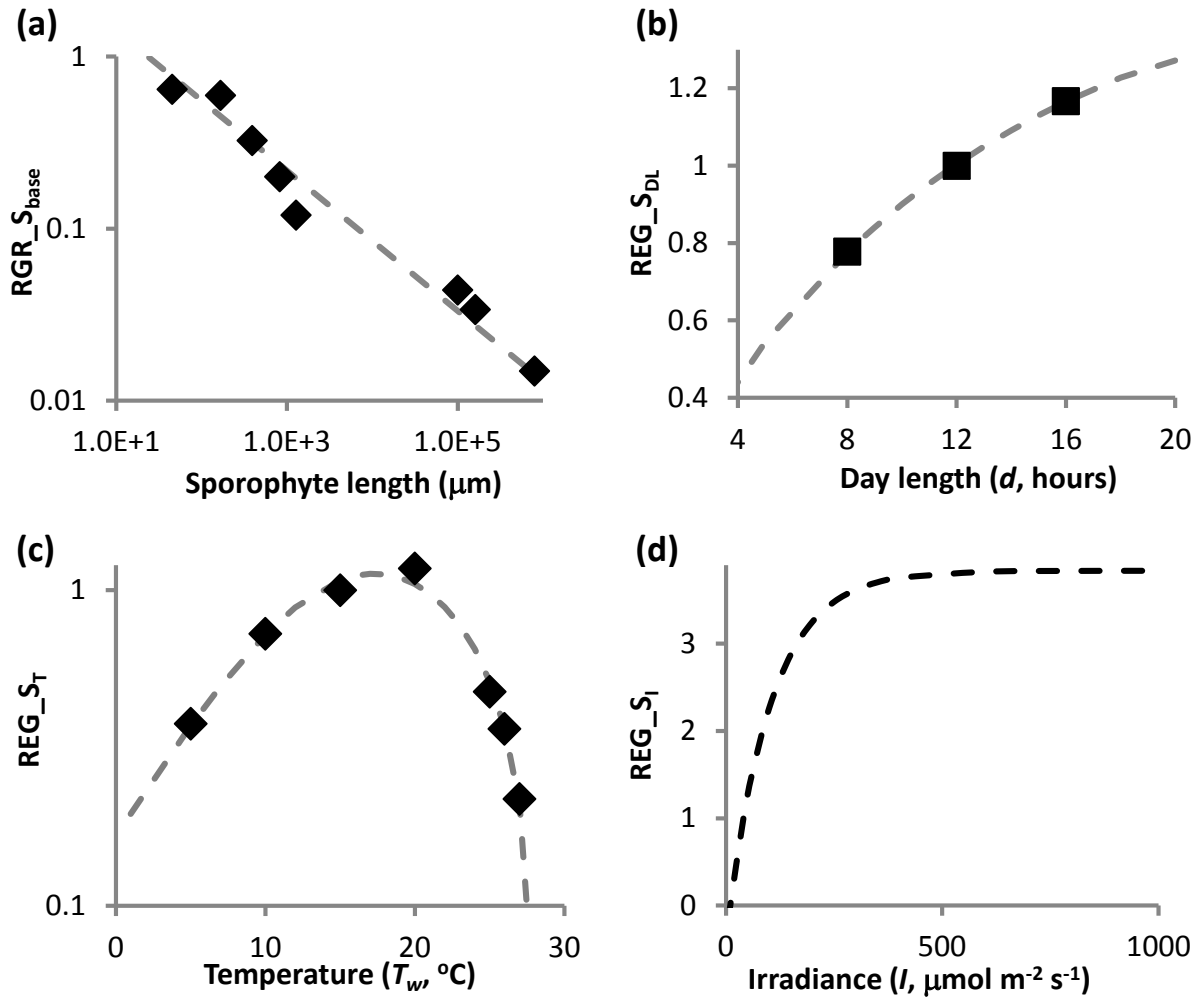

652

653 **Fig. 3:** Input data from the literature on the effects of sporophyte length and environmental
654 parameters (day light hours, water temperature and solar irradiance) on the relative growth
655 rate of *U. pinnatifida* sporophytes. ***(a)*** Power law relationship (r^2=0.97) between sporophyte
656 length and relative daily growth rate of sporophytes (*RGR_S*$_{base}$) (Pang & Wu, 1996) ***(b)***
657 Relative effect of changes in day light hours on the growth rate of sporophytes (*REG_S*$_{DL}$)
658 (Pang & Luning, 2004). Hyperbolic equation fitted to data (R^2>0.99) ***(c)*** Relative effect of
659 changes in water temperature on the growth rate (*REG_S*$_T$) of sporophytes (log scale).
660 Thermal performance fitted to data from Morita et al. (2003) (r^2>0.99). ***(d)*** Relative effect of
661 solar irradiance on the growth rate of sporophytes (*REG_S*$_I$) based on photosynthesis-
662 irradiance curve data from Campbell et al. (1999).

663

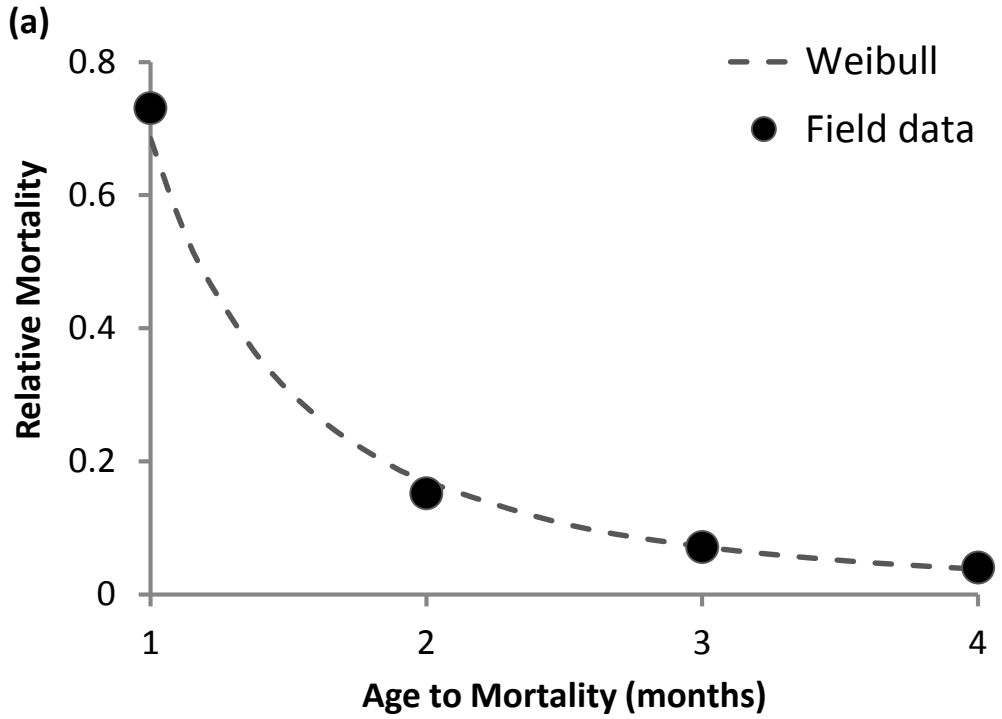

664

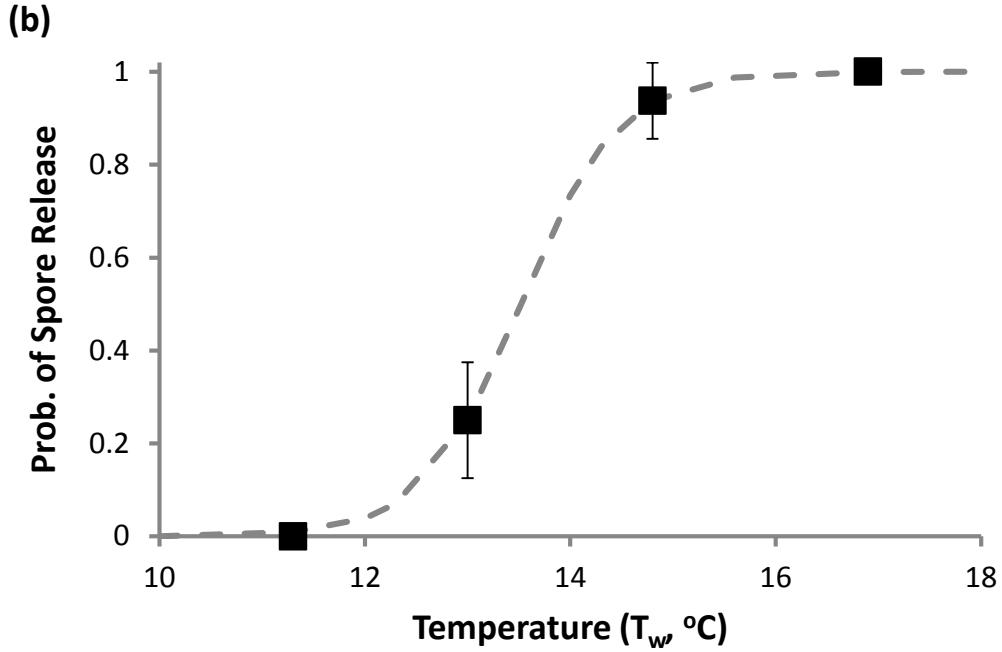

665

666 **Fig. 4: (a)** Field data on the age to mortality of immature sporophytes (n=198) growing in
667 Brest harbour surveyed in the year 2004 (Voisin, 2007). A Weibull distribution (*k*=0.1635,
668 λ=8.2E-06) was fitted to the data (R^2>0.99). **(b)** Impact of water temperature on the
669 probability of spore release from mature *U. pinnatifida* sporophytes. Logistic function fitted
670 to data from Suto (1952) (R^2>0.99).

671

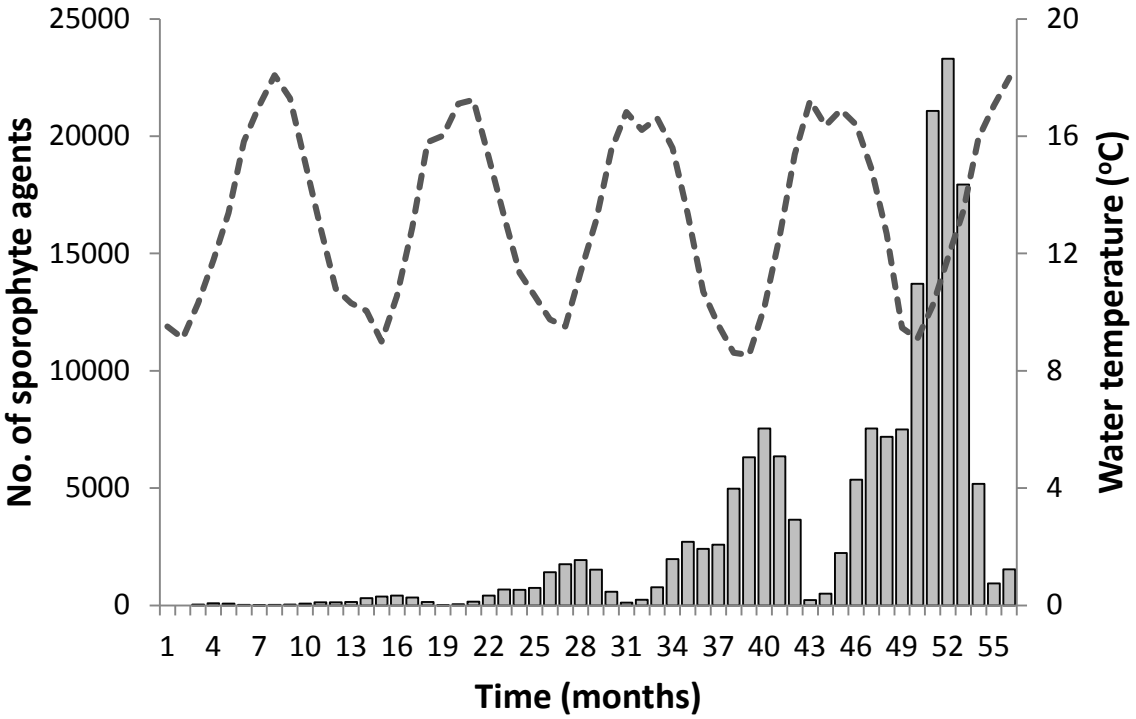

672
673 **Fig. 5:** Simulation Results: Predicted development of population of *U. pinnatifida*
674 sporophytes over the course of five seasons in environmental conditions representative of
675 Brest harbour, France. Abundance values for sporophytes are plotted on a monthly basis (bar
676 chart). Line chart represents sea water surface temperature input data (SOMLIT, Brest).
677

678 (a)

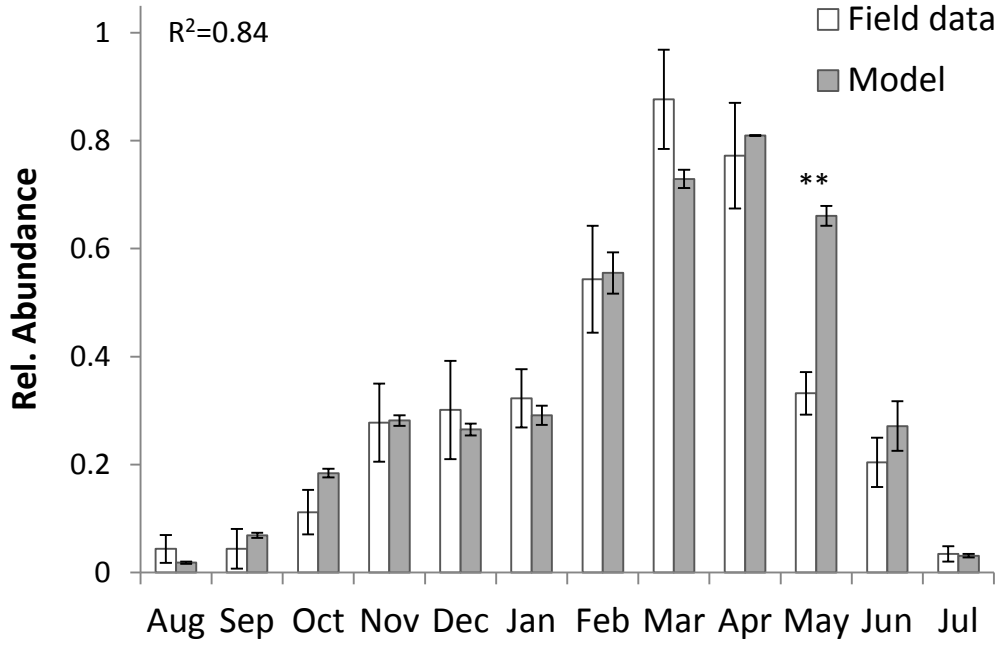

679
680 (b)

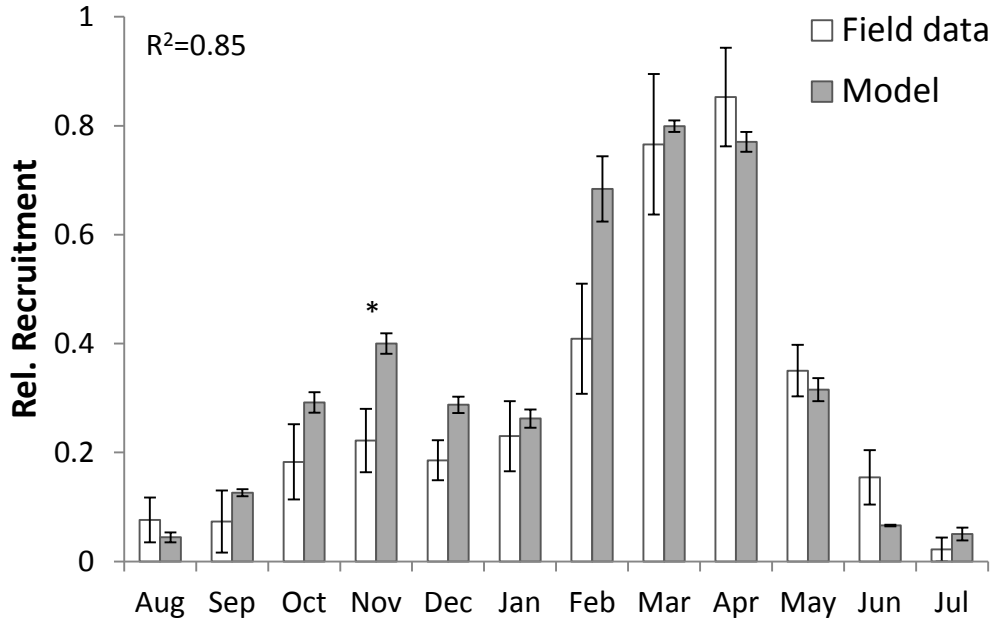

681
682
683 **Fig. 6: (a)** Predicted relative abundance and **(b)** relative rate of recruitment of *U. pinnatifida*
684 sporophytes *versus* field data from a real-world population in Brest harbour, France. Model
685 values are the means (±SE) of four simulated years. Field values are the means (±SE) from
686 five colour-coded sets of plates, installed in different locations in Brest harbour, for the
687 period Aug 2005 – Jul 2006 (Voisin, 2007).

688

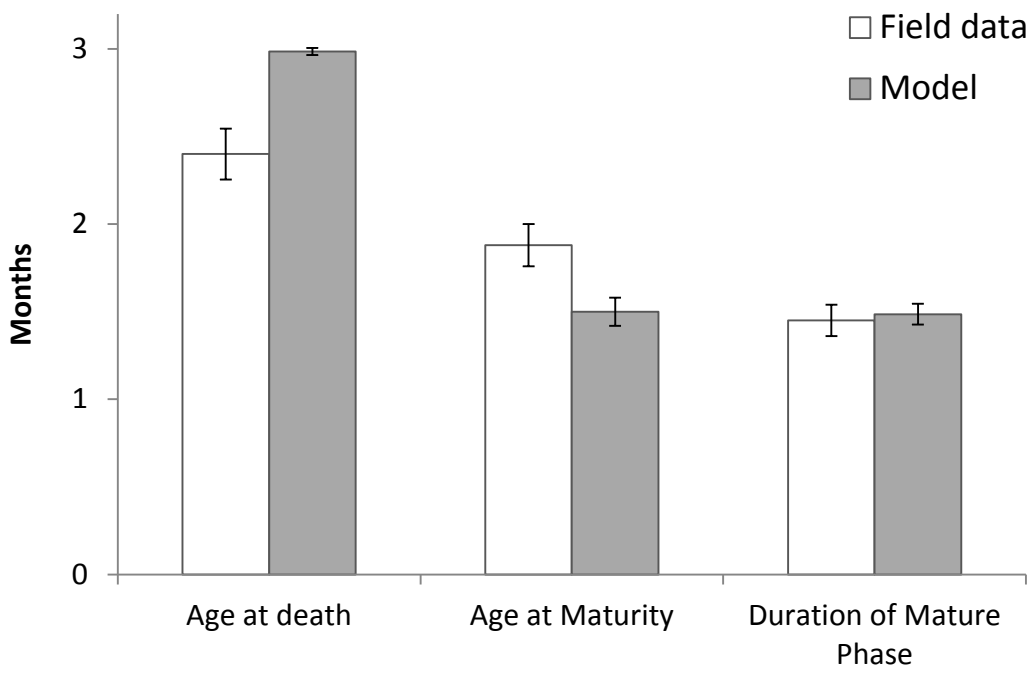

689
690 **Fig. 7:** Comparison between the predicted life expectancies of mature *U. pinnatifida*
691 sporophytes and results from field studies of a population sampled (n=94) in Brest harbour
692 over the period 2003-2006 (Voisin, 2007). The mean age at death, mean age at sexual
693 maturity (i.e. formation of sporophylls), and the number of months sexually mature (±SE) are
694 compared.

695

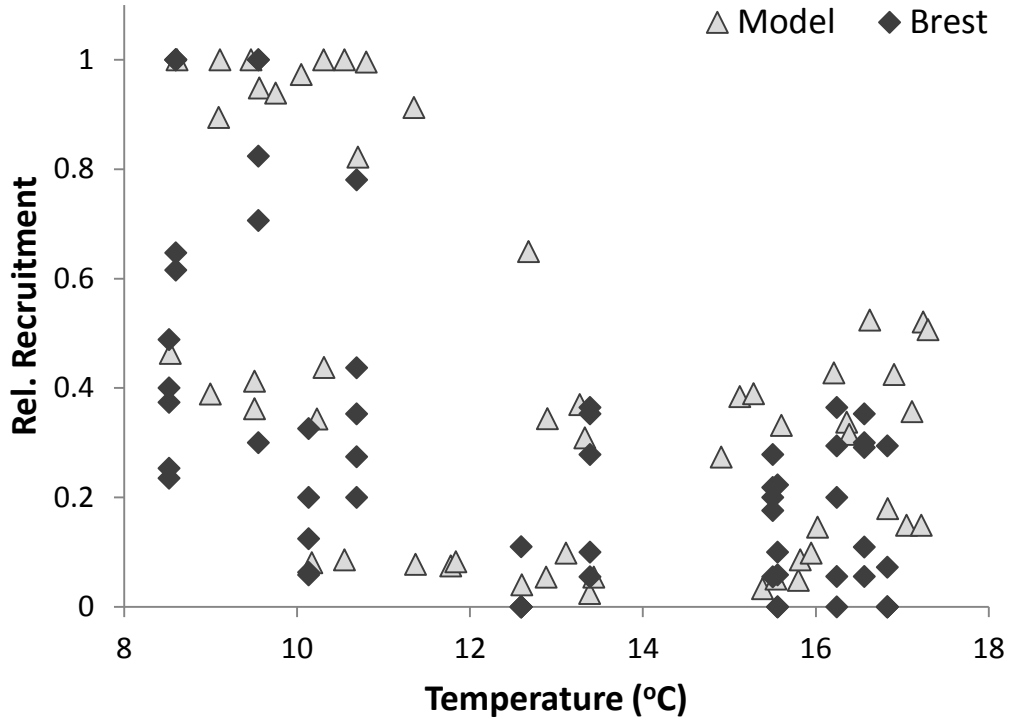

696
697 **Fig. 8:** Plot of the relationship between recruitment events (appearance of new sporophytes)
698 and water temperature for simulated *U. pinnatifida* populations. Comparison between field
699 data for the years 2003-06 (diamonds) in Brest harbour, France, and model predictions
700 (triangles).

701

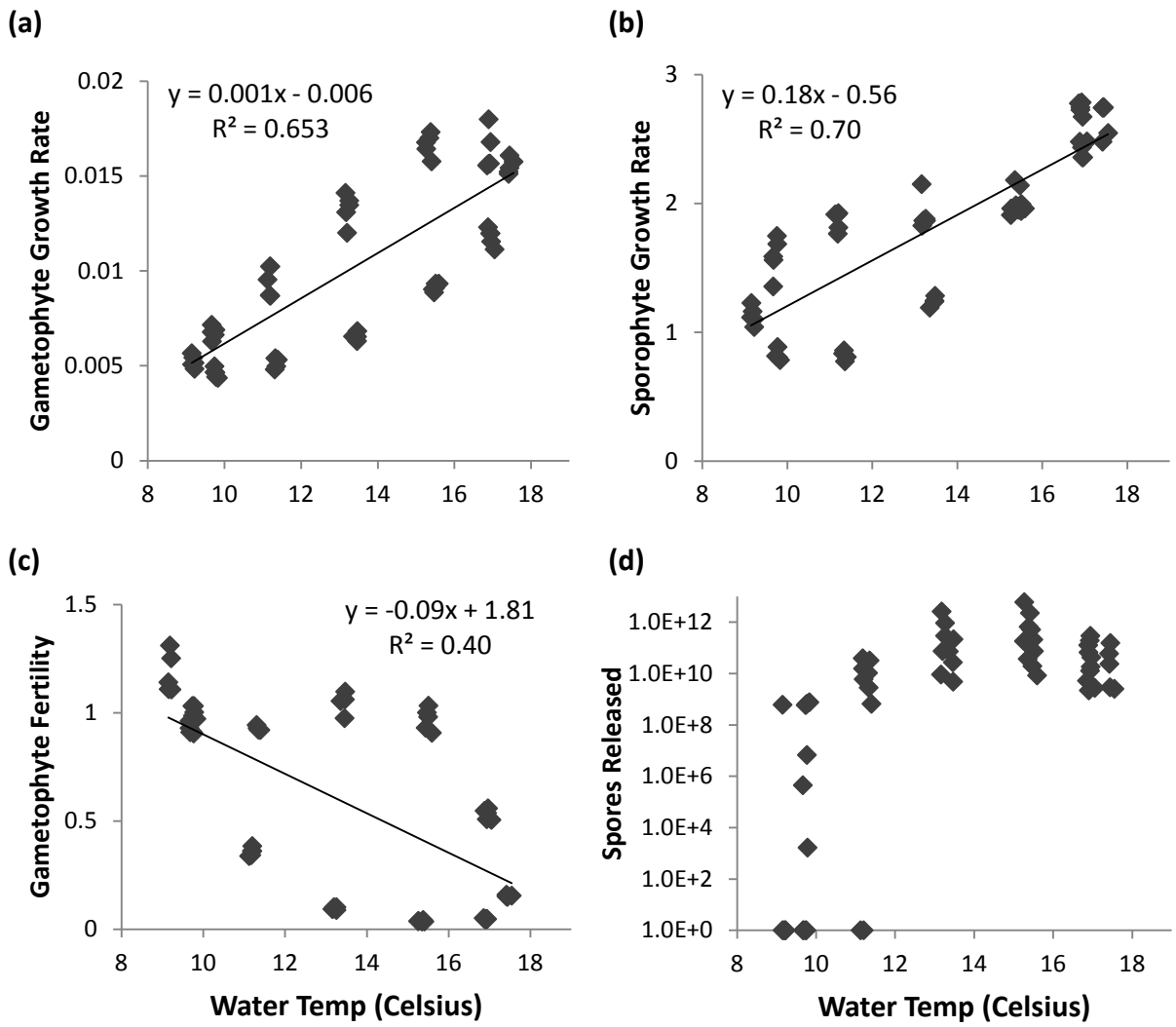

Fig. 9: Exploration of the effects of temperature on the system dynamics of the model. Relationship between water temperature and: **(a)** gametophyte growth rate, **(b)** relative sporophyte growth rate, **(c)** relative gametophyte fertility, **(d)** spores released by mature sporophytes (log scale).

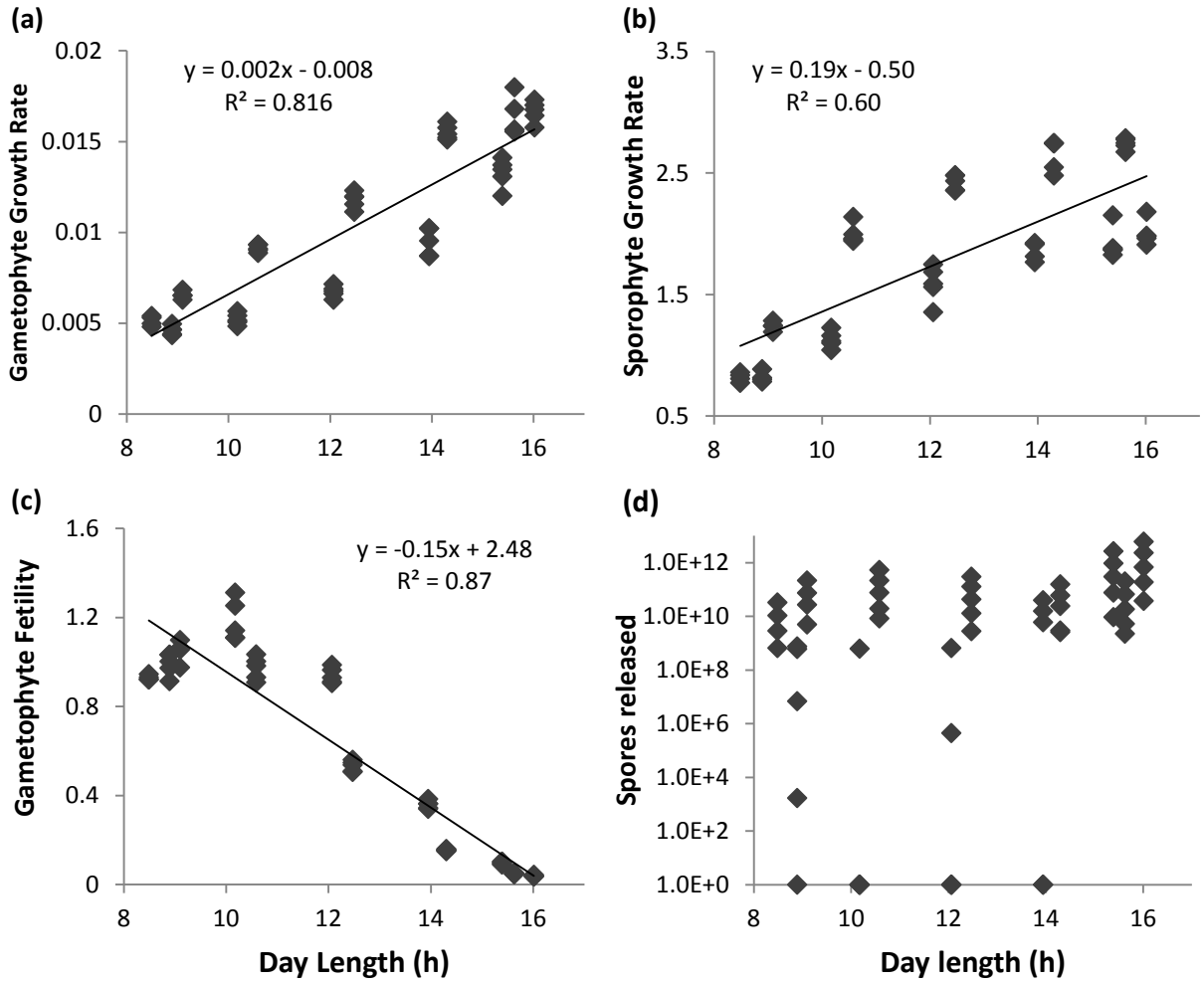

708

709 **Fig. 10:** Exploration of the effects of day light hours on the system dynamics of the model.

710 Relationship between day light hours and: **(a)** gametophyte growth rate, **(b)** relative

711 sporophyte growth rate, **(c)** relative gametophyte fertility, **(d)** spores released (log scale) by

712 mature sporophytes.

713

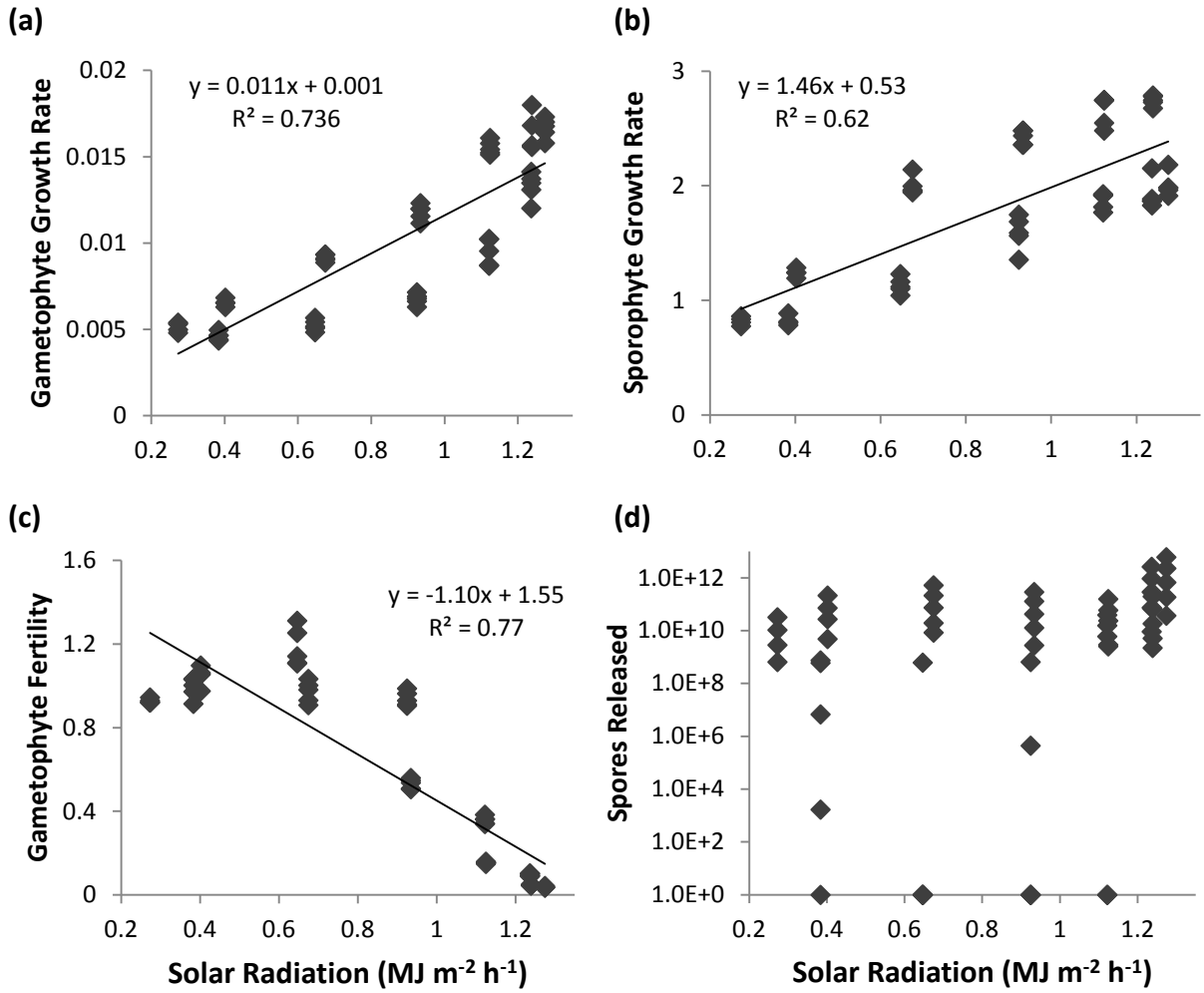

Fig. 11: Exploration of the effect of solar radiation (Megajoules m^{-2} $hour^{-1}$) on the system dynamics of the model. Relationship between day light hours and: **(a)** gametophyte growth rate, **(b)** relative sporophyte growth rate, **(c)** relative gametophyte fertility, **(d)** spores released (log scale) by mature sporophytes.

721 Table 1: Input parameters for CoastGEN simulations of *Undaria pinnatifida* in 2D simulated

722 coastal environment. l = sporophyte length (μm), d = day light hours, *loop* = simulation loop.

Parameter Type	**Parameter (units)**	**Input Value**
General	Length of Simulation Loop (hours)	1
	Environment Size (No. of Cells)	514 x 482
	Cell Area (m^2)	0.25
	Substrate depth in water (m)	1.0
	Attenuation coefficient (K_{dPAR})	0.6
Sporophyte agents	Initial length, l_0 (μm)	20.0
	Base growth rate	$3.615\ l^{-0.407}$
	Day length response (hyperbolic curve):	
	P_{max}	1.56
	a	0.13
	I_c	0.0
	Thermal performance curve :	
	K_1	21.09
	K_2	0.213
	K_3	0.006
	CT_{min}	1.62
	CT_{max}	28.28
	Scale	3031
	Photosynthesis-irradiance curve:	
	P_{max}	$0.4\ln(l) - 0.596$
	a	$0.5l^{-0.33}$
	I_c	$2.5\ln(l) – 19.9$
	Mean length at maturity (cm)	32.66
Gametophyte agents	Thermal performance curve :	
	K_1	35.67
	K_2	0.158
	K_3	0.015
	CT_{min}	4.45
	CT_{max}	28.24
	Scale	10.63

	Photosynthesis-irradiance curve:	
	P_{max}	$0.29e^{0.11d}$
	a	$0.029d - 0.2$
	I_c	0.0
	Prob. of fertilisation ($loop^{-1}$)	0.0002
Gametogenesis	Temperature response curve (log):	
	x_0	17.6
	k	0.82
	Day length response (Weibull):	
	α	4.5
	β	10.96
Spores	Half-life (hours)	24
	Release rate ($agent^{-1}$ $loop^{-1}$)	2.0×10^7
	Spore stock ($agent^{-1}$)	10^{10}
	Diffusion coefficient	0.15
	Prob. of germination ($loop^{-1}$)	10^{-9}

723